

IYI, D., BALOGUN, Y., OYENEYIN, B. and FAISAL, N. 2022. A numerical study of the effects of temperature and injection velocity on oil-water relative permeability for enhanced oil recovery. *International journal of heat and mass transfer* [online], 191, article number 122863. Available from: <https://doi.org/10.1016/j.ijheatmasstransfer.2022.122863>

A numerical study of the effects of temperature and injection velocity on oil-water relative permeability for enhanced oil recovery.

IYI, D., BALOGUN, Y., OYENEYIN, B. and FAISAL, N.

2022

A Numerical Study of the Effects of Temperature and Injection Velocity on Oil-Water Relative Permeability for Enhanced Oil Recovery

Draco Iyi^{1*}, Yakubu Balogun², Babs Oyeneyin³, Nadimul Faisal⁴

^{1*}School of Energy, Construction & Environment, Coventry University, CV1 5FB, United Kingdom
Phone: +44 (0) 2477650891, Email ac9631@coventry.ac.uk

^{2,3,4}School of Engineering, Robert Gordon University Aberdeen, AB10 7GJ, United Kingdom

Abstract

The paper quantitatively explore the influence of injection rate and temperature on oil-water relative permeability curves during hot water flooding operations in a porous medium flow. ANSYS-CFD was used to construct a numerical model of hot-water injection into an oil saturated sandstone core sample. The modelling technique is based on the Eulerian-Mixture model, using a 3D cylindrical core sample with known inherent permeability and porosity. Injection water at 20° C was injected into a core sample that was kept at 63 °C and had 14-mD permeability and 26% porosity. For the investigation, three distinct injection rates of 2.9410 - 6 m/s, 4.41×10^{-6} m/s, and 5.88×10^{-6} m/s were utilised. Furthermore, same injection procedures were repeated under the same conditions, but the core temperature was changed to 90 °C, allowing us to quantify the influence of temperature on the relative permeability curves of oil-water immiscible flow.

The results of this study show that the relative permeability of oil is strongly influenced by flow, while the effect of the relative permeability of water is negligible. In addition, the flow rate influences the residual oil and water saturation, as well as the associated effective permeability. From 20 ° C to 90 °C there is little sensitivity to relative permeability or temperature. This study does not provide proof that temperature effects do not exist with genuine reservoir fluids, rocks, and temperature ranges. However, this study has demonstrated the feasibility of utilising CFD approaches to estimate fluid relative permeability, as well as the combined influence of temperature change and flow rate on relative permeability, with the potential for considerable cost-time advantages.

Keywords: Enhanced Oil Recovery, relative permeability, Temperature effect, Injection rate, Multiphase Computational Fluid Dynamics.

Nomenclature

F	Body force
K	Permeability (m^2)
k_{eff}	effective conductivity (W/m-k)
M	Mass (kg)
P	Pressures (Pas)
Q	Flow rate (m^3/s)
S	saturations
SE	volumetric heat sources
t	Time (s)
T	Temperature (K)
V	Velocity (m/s)

Greek symbols

α	Volume fraction (dimensionless)
Σ	summation
\emptyset	Porosity (dimensionless)
μ	viscosity(kg/m-s)
ρ	density (Kg/m ³)

Subscript

o	oil
w	water
p,q,k	phase
r	relative
E	effective
dr	drift
\dot{m}	mass-average

57

58

59

60

61

62

63

64

65

66

67

68

69

70

71

72

73
74
75

1. Introduction

76 The simultaneous flow of two or more immiscible fluids occurs in a variety of natural and industrial processes,
77 including petroleum recovery, CO₂ sequestration in deep saline aquifers, environmental investigations, and
78 medication administration in biological tissues. Because two or more of water, oil, gas, and sand particles are
79 commonly produced simultaneously in the petroleum sector, transfer of fluids within the reservoir or through the
80 wellbore to surface facilities or to the refinery plant normally involves a multiphase flow scenario. A complete
81 and accurate understanding of the fluid dynamics within the domain is critical for better decision making and
82 eventual recovery when two or more immiscible fluids flow simultaneously within the reservoir or along the
83 pipeline.

84 A petroleum reservoir is a complex assemblage of porous rock, water, and hydrocarbon fluids (oil and gas)
85 that normally coexist underground at depths that make thorough measurement and characterization difficult.
86 Understanding reservoir mechanics and fluid dynamics for effective design schemes and hydrocarbon recovery is
87 a critical task for petroleum and reservoir engineers. A thorough understanding of the hydrocarbon volume in
88 place, as well as the flow conditions of the phases, is required for successful reservoir characterisation and
89 management (water, oil, gas and sand). From well drilling, completions, and production to field abandonment,
90 knowledge of reservoir mechanics and fluid dynamics supports strategic decision-making. Relative permeability,
91 capillary pressure, and wettability are three multiphase flow parameters in porous media, with relative
92 permeability being one of the most essential and critical phenomena of importance for understanding and
93 characterising the hydrodynamics inside the flow domain [1]. This convoluted pore level displacement physics,
94 as well as fluid-fluid and solid-fluid characteristics, are indicators of this complex multiphase flow behaviour in
95 a porous media [2]. These qualities are measured either in the lab or in a predictable manner utilising empirical
96 correlations or pore scale modelling.

97 It is difficult to measure porous media data that is reflective of a real-world environment. In the laboratory,
98 however, accurate modelling of all fluid and rock parameters (temperature, pressure, geometry, and composition)
99 is nearly impossible or prohibitively expensive. In order to make numerical predictions, reservoir characterization
100 entails mathematical modelling of the physical processes that occur between fluids and porous rock materials.
101 The oil and gas sector has devoted a lot of study and money to the procedures mentioned above. [3, 4, 5]. The
102 Computational Fluid Dynamics (CFD) method has been used to research and simulate multiphase flow and heat
103 transfer problems in porous media under a variety of scenarios. ANSYS-Fluent software has been adopted to
104 simulate both polymer and CO₂ flooding in a petroleum reservoir with consistent results generated which are
105 within acceptable accuracy when compared to the experiment data [6, 7, 8].
106

107 2. Review of Oil-Water Flow Relative Permeability in Porous Media

108 Laboratory approaches for measuring relative permeability are broadly classified as steady state, unsteady
109 state (dynamic displacement), centrifuge, and gravity drainage [9, 10]. Comparative examinations of these various
110 approaches have occasionally revealed discrepancies in published results, and it has been argued that the main
111 fundamentals of each method are valid under varied flow circumstances. In petroleum reservoirs, for example, a
112 single method may not sufficiently reflect the varied flow regimes in the system, necessitating the employment of
113 multiple approaches. The steady state experimental approach involves simultaneously pumping all fluid phases
114 (water, oil, and gas) into a porous media at various fixed, measurable fractional fluxes. A drawback of this method
115 is that it is difficult to achieve numerous steady states in materials with poor permeability, and there is a notable
116 influence of capillary forces and capillary end effects detected [11]. Oak, Maloney, and Brinkmeyer [12, 13] offer
117 extensive instructions for doing steady-state studies.

118 Due to the difficulties of steady-state experiments, notably the time factor, the unsteady state (also known as
119 dynamic displacement) technique has been widely employed in the literature for relative permeability
120 investigations. In this example, only one fluid is injected into the core sample, and data on the pressure decrease
121 across the sample and phase recovery is collected. Despite its widespread use and applications, there are
122 significant limitations that contribute to certain fundamental assumptions made in its implementation. The method
123 is not appropriate for studies with low flow rates and a substantial influence of capillary pressure. High flow rates,
124 on the other hand, may enhance the occurrence of viscous fingering, which refers to the creation of an uneven
125 finger-like pattern at the interface of two fluids, such as oil and water [14]. According to Singh [15], the unsteady-
126 state approach is thus more suited for flow circumstances characterised by large front velocity displacements.

127 Analytic, semi-analytic, and numerical/history-matching approaches are used to analyse relative permeability
128 experimental data [16].

129 Arshad [17] reported experimental research on the temperature impacts on oil-water relative permeability,
130 with the findings suggesting that the relative permeability curves, as well as the endpoint saturations, are
131 temperature independent. Miller and Ramey Jr. [18] made the same observation after doing dynamic-displacement
132 laboratory tests on unconsolidated and consolidated porous medium using water and a refined white mineral oil
133 to assess relative permeability to oil and water. The trials were carried out on 5.1 cm diameter and 52 cm long
134 cores at temperatures ranging from ambient temperature to about 149 °C. The results presented demonstrate that
135 the relative permeability curves largely do not vary with temperature fluctuation. They claimed that prior
136 published results might have been influenced by variables such as viscosity instabilities, capillary end effects, or
137 a potential difficulty in maintaining material balances.

138 To examine the link between relative permeability curves and temperature, Lie-hui *et al.*, [19] performed a
139 series of core flooding tests on five sandstone core samples with varying permeability values at various
140 temperatures. Given that laboratory circumstances cannot completely replicate fluid flow behaviour in a reservoir,
141 they suggested a method for translating laboratory results to reservoir size. The study discovered a substantial
142 increase in the form of oil and water relative permeability curves as temperature increased for the various core
143 samples and permeability ranges. With increasing temperature, residual oil saturation decreased nonlinearly, but
144 irreducible water saturation rose linearly but decreased with decreasing permeability. Akhlaghinia *et al.* [20],
145 utilised heavy oil, methane, and carbon dioxide to evaluate relative permeability in sandstone core samples, and
146 the JBN method to compute two-phase relative permeability. To study the influence of temperature on the form
147 of relative permeability curves, a series of tests were carried out at three distinct temperature values of 28, 40, and
148 52 °C for different fluid pairs. The oil relative permeability curve rose at a rate of approximately 70% with a
149 temperature change from 28 to 40 °C and dropped at a rate of about 30% with a temperature change from 40 to
150 52 °C, according to the experimental data. The study concluded that at a particular temperature, the relative
151 permeability trend reverses, indicating that the oil relative permeability varies up to an optimal temperature of
152 about 40 to 52 °C, after which the trend reverses with further increase in temperature. Bennion *et al.* [21]
153 demonstrated a relationship between temperature and oil-water relative permeability in unconsolidated bitumen
154 producing strata in Canada. The study was a thorough examination of current field oil-water relative permeability
155 data collected at temperatures ranging from 10 to 275 °C in order to show correlations for predicting oil-water
156 relative permeability features and residual oil saturations (mainly for preliminary evaluation analysis). It was
157 observed that when temperature rises, residual oil saturation falls in a non-linear fashion while water saturation
158 rises. At temperatures less than 100 °C, the relative permeability to brine was shown to be sensitive.

159 Torabi *et al.* [22] conducted a series of unsteady state core flooding experiments to investigate the effect of
160 various vital fluid flow parameters such as operating temperature, oil viscosity, injection rate, and pressure on oil-
161 water relative permeability, and new correlations for computing oil-water relative permeability were proposed.
162 According to the findings of this investigation, the relative permeability of water and oil increases considerably
163 as temperature rises. A decrease in oil viscosity was shown to result in an increase in permeability to oil and water.
164 Behnam *et al.* [23] conducted unsteady state core flood tests on core samples from carbonate reservoirs under
165 reservoir pressure conditions and original fluid saturations at high temperatures ranging from 38 to 260 °C. The
166 data from the tests were analysed using history matching and the JBN technique, with the findings indicating that
167 the relative permeability of both fluids is a function of temperature. Possible wettability changes at increasing
168 temperatures were proposed to have resulted in a shift in the oil relative permeability curve as temperature
169 increased. This study contradicted earlier studies utilising sandstone core samples, which found that increasing
170 temperature causes residual oil saturation to decrease while increasing irreducible water saturation. More recent
171 studies on temperature dependent oil-water relative permeability were carried out by Esmacili *et al.* [24, 25] on
172 water-bitumen system under temperature range of 70 to 220 °C and confining pressure of 1400 psi and reported
173 that both oil and water relative permeability is temperature sensitive. The same authors [26] carried out similar
174 sets of experiments under different operation conditions. Under temperature of between 23 °C and 210 °C with
175 confining pressure of 800 psi for light oil of viscosity between 11.2 – 2281 cP, the study revealed that oil/water
176 relative permeability is insensitive to temperature. The difference reported in both studies can be attributed to the
177 complex rock-fluid system with features such as wettability and interfacial tension varying for the bitumen-rock
178 system compared to the clean oil-rock system.

179 While ample research efforts have been put into studying temperature dependent relative permeability, there
180 is lack of consensus on the effect as reported by Esmacili *et al.* [27]. A key fact worth noting is that relative
181 permeability is only sensitive to temperature fluctuation in specific temperature ranges. The pattern then reverses
182 when the temperature increases more. While some investigators maintained that there are some modifications

183 without recognising the optimal temperature, others claimed that there is no difference. The results of the
184 experimental literature assessment and analysis do not clearly show a consistent trend between relative
185 permeability and temperature. It is consequently important to examine the temperature dependence of relative
186 permeability curves, although using numerical modelling using computational fluid dynamics software rather of
187 practical experimentation.

188 Although theoretical or analytical methods for fluid mechanics and heat transfer have been established,
189 multiphase flow modelling requires the solution of second-order partial differential equations, which are
190 analytically intractable. This is due mostly to the intrinsic nonlinearity of the flow equations for multiphase
191 porous-media flow issues [28, 29, 30]. The major reason for using a CFD experimental technique is that it is less
192 time-consuming and expensive while providing capabilities that cannot be explored in a laboratory [31]. To help
193 in the research of flow characteristics in porous medium, specialised software programmes, both commercial and
194 open source, have been created in the field of CFD. Glatzel *et al.* [32] conducted comparative research on the
195 applicability of four main commercial CFD software (Fluent, CFD-ACE, CFX, and Flow-3D) in flow simulations
196 via micro channels and capillary structures and showed the usefulness of these software for various parameter
197 investigations. Despite the fact that the usage of these CFD programmes has been established in these domains,
198 the majority of the research have been focused on studying flow phenomena in micro-channels. Other research
199 on macroscopic characteristics in porous media has been done [33, 34, 35].

200 The models essentially include the inclusion of the Darcy-Forcheimer equations as source terms in the
201 momentum equations, which have been utilised to account for various system characteristics, including
202 permeability and pressure drop in single-phase and multiphase flow regimes. Li *et al.* [33] demonstrated the
203 capabilities of ANSYS® Fluent CFD software for modelling multiphase flows in porous media, with a particular
204 emphasis on reservoir and well performance studies. To simulate reservoir and well conditions, oil-water flow
205 was modelled in 1D, 2D, and 3D geometries. The numerical methodology used in this work is the Eulerian
206 multiphase multi-fluid method in Fluent with a time-step and grid independent result, demonstrating the enormous
207 potential of employing ANSYS-Fluent software for practical reservoir and well performance analysis.

208 To the best of our knowledge, no work in the open literature has used a CFD technique to evaluate relative
209 permeability in a displacement flow scenario. Because multiphase flow in porous media is a complicated process,
210 the complexity involved in include relative permeability and capillary pressure in the CFD solver might explain
211 this result. Because relative permeability is a function of saturation, when the fluid saturation in the cells
212 approaches irreducible values and relative permeability approaches zero, numerical instabilities in the CFD solver
213 may occur if the relative permeability and capillary pressure are included in the solver [33].

214 In this work, a hot water injection procedure was performed in the Fluent CFD solver to model a thermal
215 recovery process, and flow results from the solver were utilised to determine relative permeability by using
216 multiphase equations derived from Darcy's equation. The scenario studied in this paper is a typical tertiary oil
217 recovery operation in which hot water is pumped into the reservoir to lower the viscosity of the oil, therefore
218 improving oil mobility and, ultimately, recovery. The final goal of this research is to investigate the influence of
219 temperature and injection rate on relative permeability curves during hot water flooding operations. The examined
220 simplified model includes a temperature-dependent two-phase (oil-water) flow through a porous medium
221 associated with heat transfer.
222

223 3. Problem descriptions

224 ANSYS-Fluent was used to create a three-dimensional model of a cylindrical core sample with a diameter of
225 3.8 cm and a length of 12 cm. As indicated in Figure 1, the model boundary condition comprises of the inlet face,
226 outflow face, and wall body. Instead of specifying the shape and direction of each solid matrix within the porous
227 body, the flow is described as a continuous process utilising average or "continuous" characteristics for the bulk
228 system as a convention for a macroscopic description of fluid flow in the subsurface. The average flow rate for
229 the total volume is calculated by plugging the bulk characteristics into the traditional Darcy's equation. The
230 computational domain was built up to imitate the thermal recovery process with the injection of hot water from
231 the inlet using specified operating settings to explore the influence of temperature and injection rate on relative
232 permeability curves during water flooding. The processes were computationally simulated, and the relative
233 permeability was calculated using multiphase equations derived from Darcy's equation. A mesh sensitivity
234 analysis was performed, and all of the results presented in this paper used a structured mesh with an orthogonal
235 quality of 1.

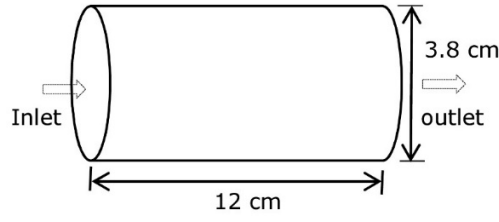


Figure 1: Schematic of the flow domain.

236
237
238

239 4. Numerical Method

240 This section shows how to solve a problem involving the flow of two incompressible and immiscible fluids,
241 oil and water, which are denoted by the letters o and w , respectively. The porous media is believed to be
242 incompressible and homogeneous. The equations for Mass conservation equation (Eq.1) and generalised
243 Darcy's law for multiphase flow (Eq.2) [36, 31, 37].

$$\begin{cases} \frac{\partial}{\partial t}(\phi \rho_w S_w) + \nabla(\rho_w v_w) = -Q_w \\ \frac{\partial}{\partial t}(\phi \rho_o S_o) + \nabla(\rho_o v_o) = -Q_o \end{cases} \quad (1)$$

244

$$\begin{cases} v_w = -\frac{K k_{rw}}{\mu_w} (\nabla P_w - \rho_w g) \\ v_o = -\frac{K k_{ro}}{\mu_o} (\nabla P_o - \rho_o g) \end{cases} \quad (2)$$

245
246
247
248
249
250
251
252

Because both phases are incompressible, the fluid densities ρ_w and ρ_o are constant in the flow domain, and the petro-physical parameters of the media, such as porosity and permeability, are pressure independent. The following relationship must be met by the fluid saturations: $S_w + S_o = 1$ where $S_{wi} \leq S_w \leq 1 - S_{or}$ and $S_{or} \leq S_o \leq 1 - S_{wi}$. There will be no flow at water saturations below the irreducible water saturation (S_{wi}), and the oil phase will become immobile at oil saturations below the irreducible oil saturation (S_{or}). Under the premise that water is the wetting phase, the relationship for capillary pressure as a function of wetting phase saturation relates both fluid pressures; the correlation is stated as:

$$P_c(S_w) = P_o - P_w \quad (3)$$

253
254

The capillary pressure drops as the water saturation decreases. Equation 4 below are obtained by combining equations 1, 2 and 3.

$$\begin{cases} \frac{\partial}{\partial t}(\phi S_w) + \nabla\left(-\frac{K k_{rw}}{\mu_w} (\nabla P_o - \nabla P_c - \rho_w g)\right) = -Q_w \\ \frac{\partial}{\partial t}(\phi S_o) + \nabla\left(-\frac{K k_{ro}}{\mu_o} (\nabla P_o - \rho_o g)\right) = -Q_o \end{cases} \quad (4)$$

255
256
257

4.1. Relative permeability

258
259
260
261
262

There is some blockage of flow on a given fluid phase by other fluid phases present in the system in multiphase flow in porous media where two or more fluids flow concurrently, and this is represented by a scalar called relative permeability. The ratio of the phase effective permeability ($K_{e,q}$) to the media's absolute permeability, K , is the relative permeability of a fluid phase q . The relative permeability K_r of the fluid phase q can be represented as:

$$K_{r,q} = K_{e,q} / K \quad (5)$$

263
264

The relative permeability K_r is a dimensionless number with a value between 0 and 1, whereas the absolute permeability K , with a dimension in m^2 , represents the ability of porous media to transport a single saturated fluid

265 and is only dependent on the geometric properties of the pores. The permeability of the phase q in a multiphase
 266 system, or the ability of the media to transport the fluid phase q in the presence of other fluid phases is known as
 267 the effective permeability K_e , and it is influenced by the media's absolute permeability and phase saturation
 268 (volume fraction). Equations (2) and (5) clearly shows the relationship between the absolute permeability and the
 269 relative permeability in any porous media flow and were employed to evaluate the relative permeability in the
 270 two-phase porous media flows in this study.

271 Throughout the transient flow simulation, the sample average saturation for each fluid phase, as well as the
 272 pressure drop and flow rates were continuously monitored. The values of the input parameters at different flow
 273 times and water saturation were determined after a series of simulations for the different parameters of interest.
 274 We assumed a significant temperature dependence of the oil viscosity in our simulations in this study, and the
 275 power law model developed by Corey was used to predict the two-phase relative permeability. Equation (6) and
 276 (7) depicts the classical Corey model.

$$K_{rw} = K_{rw(S_{orw})}(S)^{N_w} \quad (6)$$

$$K_{ro} = K_{ro(S_{wi})}(1 - S)^{N_o} \quad (7)$$

278 Where, K_{rw} and K_{ro} are the relative permeability to water and oil respectively. $K_{rw}(S_{orw})$ and $K_{ro}(S_{wi})$ are the
 279 endpoint relative permeability to water at residual oil saturation(S_{or}) and oil at initial water saturation (S_{wi})
 280 respectively. N_w and N_o are the Corey exponent to water and oil respectively. The values 4 and 2 have been used
 281 for the water and oil exponent respectively as indicative of a water-wet porous media [22, 38]. In addition, S in
 282 the Equation (6) and (7) is typically represented in normalised form as shown in Equation (8).

$$S = \frac{S_w - S_{wi}}{1 - S_{wi} - S_{orw}} \quad (8)$$

283 Where, S_w is water saturation, S_{wi} is initial water saturation and S_{orw} residual oil saturation. Following each
 284 set of simulations, both the water saturation and residual oil saturation were recorded in the volume fraction under
 285 the ANSYS-Fluent report section.

286 4.2. Mixture model

287 The primary idea of mixture theory is that the constituents that make up the mixtures are assumed to occupy
 288 the vacuum or pore spaces occupied by the fluid mixture, and each of them is treated as a continuum at each point
 289 within the medium filled with the mixture. The contributions of mass, momentum, and energy within the flow
 290 domain are considered relative to the effect of other elements, according to the conservation laws of mass,
 291 momentum, and energy. The mixture model is a condensed version of the multiphase model, which can simulate
 292 multiphase flow systems with various phases moving at different velocity yet assuming local equilibrium over
 293 short spatial length scales.

294 The continuity, momentum, and energy of the mixture are calculated, while the volume fraction of the
 295 secondary phase(s) is solved, as well as algebraic formulations for relative velocities in flows when the phases
 296 move at different velocities. The mixture model was chosen because it is less computationally costly than the full
 297 multiphase flow model in terms of solving the multiphase flow governing equations in less time. Its shortcoming
 298 is that it does not account for the pressure of individual phases; instead, it only accounts for the pressure of the
 299 mixture, making capillary pressure estimates impossible. CO_2 injection [7], Nano-fluid flooding [39], thermal
 300 recovery [40] and chemical flooding [41] are only a few of the multiphase flow challenges for which this model
 301 has been used. The Fluent model solves the following governing equations [37]:

302 Continuity equation for the fluid mixture

$$\frac{\partial}{\partial t}(\rho_m) + \nabla \cdot (\rho_m \vec{v}_m) = \dot{m} \quad (9)$$

303 Where \vec{v}_m is the mass-averaged velocity expressed by $\vec{v}_m = (\sum_{k=1}^n \alpha_k \rho_k \vec{v}_k) / \rho_m$ and ρ_m is the mixture
 304 density given as, $\rho_m = \sum_{k=1}^n \alpha_k \rho_k$, where α_k is the volume fraction of the phase k and m is the mass sources.

305 Momentum equation for the mixture

$$\begin{aligned} \frac{\partial}{\partial t} (\rho_m \vec{v}_m) + \nabla \cdot (\rho_m \vec{v}_m \vec{v}_m) \\ = -\Delta p + \Delta \cdot [\mu_m (\nabla \vec{v}_m + \Delta \vec{v}_m^T)] + \rho_m \vec{g} + \vec{F} + \Delta \cdot \left(\sum_{k=1}^n \alpha_k \rho_k \vec{v}_{dr,k} \vec{v}_{dr,k} \right) \end{aligned} \quad (10)$$

306 Where n is the number of fluid phases, viscosity of the mixture represented as μ_m and body force \vec{F} . The drift
307 velocity for the secondary phase in the mixture represented as $\vec{v}_{dr,k} = \vec{v}_k - \vec{v}_m$. The velocity of the secondary
308 phase (p) relative to the primary phase (q) otherwise referred to as relative or slip velocity is given by $\vec{v}_{qp} = \vec{v}_p -$
309 \vec{v}_q .

310 Energy equation for the mixture

$$\frac{\partial}{\partial t} \sum_{k=1}^n (\alpha_k \rho_k E_k) + \nabla \cdot \sum_{k=1}^n (\alpha_k \vec{v}_k (\rho_k E_k + p)) = \nabla \cdot (k_{eff} \nabla T) + S_E \quad (11)$$

311 Where k_{eff} represents the effective conductivity and S_E represents any other volumetric heat sources.

312 According to Mohammadmoradi et al. [42] accurate operation of the thermal increase oil recovery method
313 requires knowledge of the heat transmission mechanism in a porous media. Effective heat helps to reduce fluid
314 viscosity, which improves mobility and thus recovery. Effective thermal conductivity (ETC) and effective thermal
315 diffusivity (ETD) are the two key core characteristics used to determine how effective thermal energy may be
316 conveyed in a porous media. Furthermore, shape, porosity, and fluid saturation all have an impact on effective
317 thermal conductivity [5]. The flow velocity is a crucial component in determining a non-isothermal condition in
318 a system. In the case of the slow flow system discussed in this study, the distinct phases may interact and exchange
319 energy locally to achieve a condition of local thermal equilibrium. A single energy equation is required in this
320 situation to represent the temperature of all phases inside the domain at any given position. Coupling allows for a
321 strong relationship between oil viscosity and temperature.

322

323 4.3. Operating conditions and assumptions

324 With initial water saturation S_w and initial oil saturation S_o , the displacement of oil with water in the
325 consolidated cylindrical homogeneous porous core of porosity \emptyset . For the flow inside the porous media,
326 incompressible laminar bi-phasic flow is examined. Between the fluids and the porous body, the local thermal
327 equilibrium (LTE) assumption is considered valid. The following assumptions were considered when building the
328 model:

- 329 ▪ To displace the oil in the initially heated porous core, the porous core was injected with hot water at a
330 steady rate and at a specified temperature at the intake face.
- 331 ▪ It is assumed that the medium is isotropic, having the same flow in all three directions.
- 332 ▪ The fluid viscosity can vary with temperature with the input done through the piecewise linear property
333 input.
- 334 ▪ With the same density, the fluids are incompressible, but at different pressures and temperatures.
- 335 ▪ Petrophysical qualities of rocks, such as porosity and permeability, are thought to be constant and
336 unaffected by pressure or temperature.

337 The effect of injection rate and injection fluid temperature on fluid relative permeability in a convectional
338 core flooding system is explored in this paper. Three different velocities (2.94×10^{-6} m/s, 4.41×10^{-6} m/s, and
339 5.88×10^{-6} m/s), as well as temperatures (20 and 70 °C) were simulated at the intake, with the core temperature set
340 at 63 °C. The simulation input settings were chosen to be typical to core flooding laboratory experiment reported
341 by Ahmadi et al., [43]. Prior to the start of the water injection, the model was set to a 20 percent water saturation.
342 The water and oil phases have densities of 998.2 and 730 kg/m³, respectively. The water phase's viscosity is
343 0.001003 kg/m-s, while the oil phase's is temperature dependant (Fig. 2). The parameters of the fluid and porous
344 media employed in this study are summarised in Table 1.

345 The physical characteristics of the system, as well as the operating conditions, has been designed in order to
346 maintain the flow as a two-phase flow in a relatively low temperature petroleum reservoir. It is worth noting that
347 because the ambient pressure condition was considered in the modelling, at temperatures above 100 °C, the liquid
348 phase will change to vapour phase, giving rise to a three-phase flow, which is not the intention of this study. As a
349 result, a low temperature was considered. Furthermore, we chose this range because it is representative of reservoir
350 temperature in low-temperature petroleum reservoirs. Additionally, this is the temperature condition in the

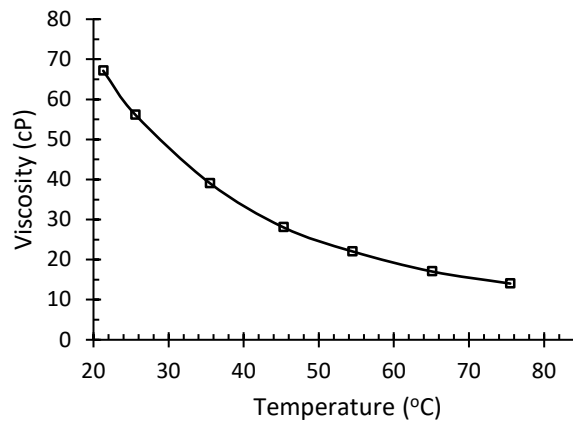
351 experimental benchmark study that was used as validation for this study. In particular, in the simulations, it was
 352 modelled as incompressible flow, with the density remaining constant in any fluid parcel. This is primarily due to
 353 the fact that no confining pressure was applied, resulting in an ambient pressure condition. Under these conditions,
 354 it is widely accepted that the liquid phase is nearly incompressible. Water, for example, is easily compressible
 355 in the vapour phase (steam), but the simulations did not reach the temperature of 100 °C required for this to
 356 happen. We mentioned earlier that liquids are generally incompressible, but they are compressible if the pressure
 357 is high enough.

358 The concept of hysteresis has been neglected in this study, as the simulation is entirely an imbibition scenario.
 359 Typically, in a reservoir, relative permeability hysteresis is evident whenever a media with strong wettability
 360 preference experiences a change in saturation from a drainage to an imbibition process. However, in this study,
 361 there is no history of moving from drainage to imbibition in the workflow. In addition, as reported by Mobeen
 362 and Mehran [44] in a scenario where the reservoir is depleted by a reduction in the oil saturation and a
 363 corresponding increase of the wetting phase saturation (water), the imbibition relative permeability curves must
 364 be applied.
 365
 366
 367

Table 1: Model parameters for Media properties.

Porous media property	Value	Porous media property	Value
Length (cm)	12.0	Initial Water Saturation (S_{wi}) (%)	20.0
Diameter (cm)	3.8	Pore volume (cc)	35.0
Porosity (%)	26.0	Thermal conductivity (W/m-k)	2.25
Permeability (mD)	14.0		

368



369

Figure 2: Oil viscosity variation with temperature.

370

371

372 5. Results and Discussion

373 This section examines the numerical results of temperature and injection rate effects on relative permeability.
 374 The oil-water saturation profiles at various flow periods and at varied sample lengths of 0.2 increments starting
 375 from the intake are given in section 5.1, along with validation of the numerical methods against recovery factor
 376 data adapted from a core flood experiment [43]. In section 5.2, the effects of temperature and injection velocity
 377 on the oil-water relative permeability are discussed.
 378

379 5.1. Validation of the numerical method and Oil-water saturation profiles

380 Figure 3 shows a simplified schematic of the experimental set-up modified from Ahmadi et al., [43]. In Figure
 381 4, the recovery factor results from the current investigation were plotted against the core flooding experimental
 382 data at various time intervals. The numerical values used in the validation analysis are identical to the experimental
 383 conditions without calibration of the physical or numerical modelling parameters, except for the fluid viscosity
 384 dependence on temperature, which was incorporated as an interpreted User-Define-Function in ANSYS-Fluent,
 385 with injection temperature of 20 °C and inlet velocity of 2.94×10^{-6} m/s. With a smaller than ± 2.5 percent error
 386 margin, the results show a positive comparability between numerical and experimental data.

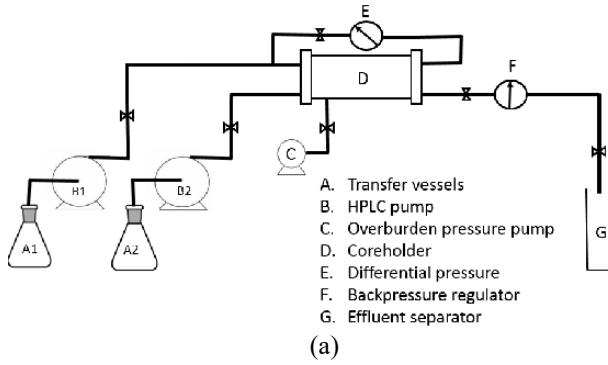


Figure 3: Experimental set-up used for numerical results validation. Ahmadi et al., [43].

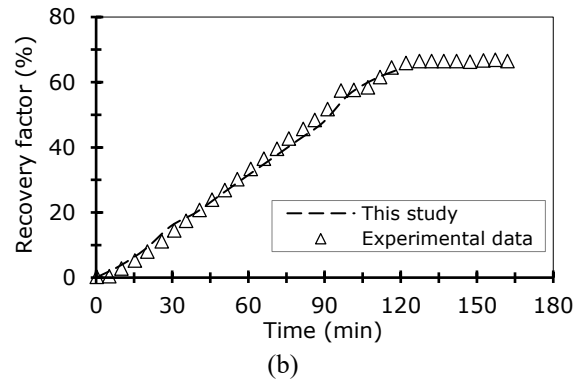


Figure 4: Experimental and numerical simulation recovery factor plot.

387 In Figure 4, the recovery factor calculated from the simulation is compared to results from a core flooding
 388 experiment published in the literature. The injection temperature and flow rates are modified based on the
 389 simulation and experiment results and the data is used to compute relative permeability curves to explore the
 390 sensitivity of relative permeability to temperature and injection flow rate. Figure 5 shows the water saturation
 391 (volume fraction) along the length of the core sample at various time intervals. With an inlet velocity of 2.94×10^{-6}
 392 m/s, the oil and water volume fractions are zero and one at the commencement of the injection. In section 4.3,
 393 the fluid and porous media properties, as well as the initial flow conditions, are described.

394 The frontal advance profile volume-fraction curves often follow the linear Corey model, which has a zero
 395 residual saturation and a phase relative permeability of unity. It can be seen that when the injected water's
 396 saturation time increases from 5 to 85 minutes, it permeates a considerably larger section of the porous core at a
 397 faster rate. This could be owing to the relative permeability of the two fluids when they interact with one other,
 398 as predicted by the model's assumptions. In the core domain where displacement has occurred, the results also
 399 revealed an absolute oil saturation value of zero and a water saturation value of one. This is not the case in actual
 400 displacement processes, where some slippage will occur as irreducible saturation at the solid surface.

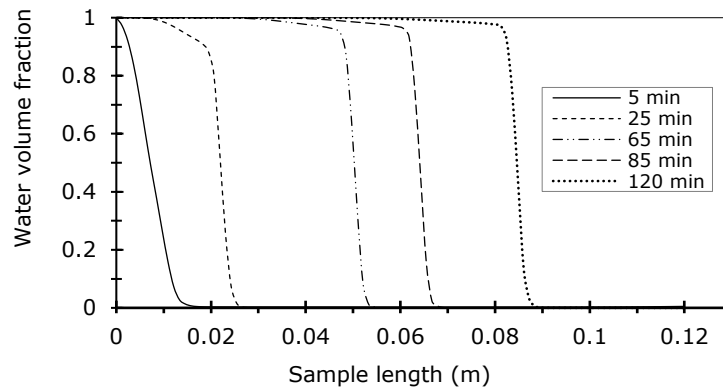
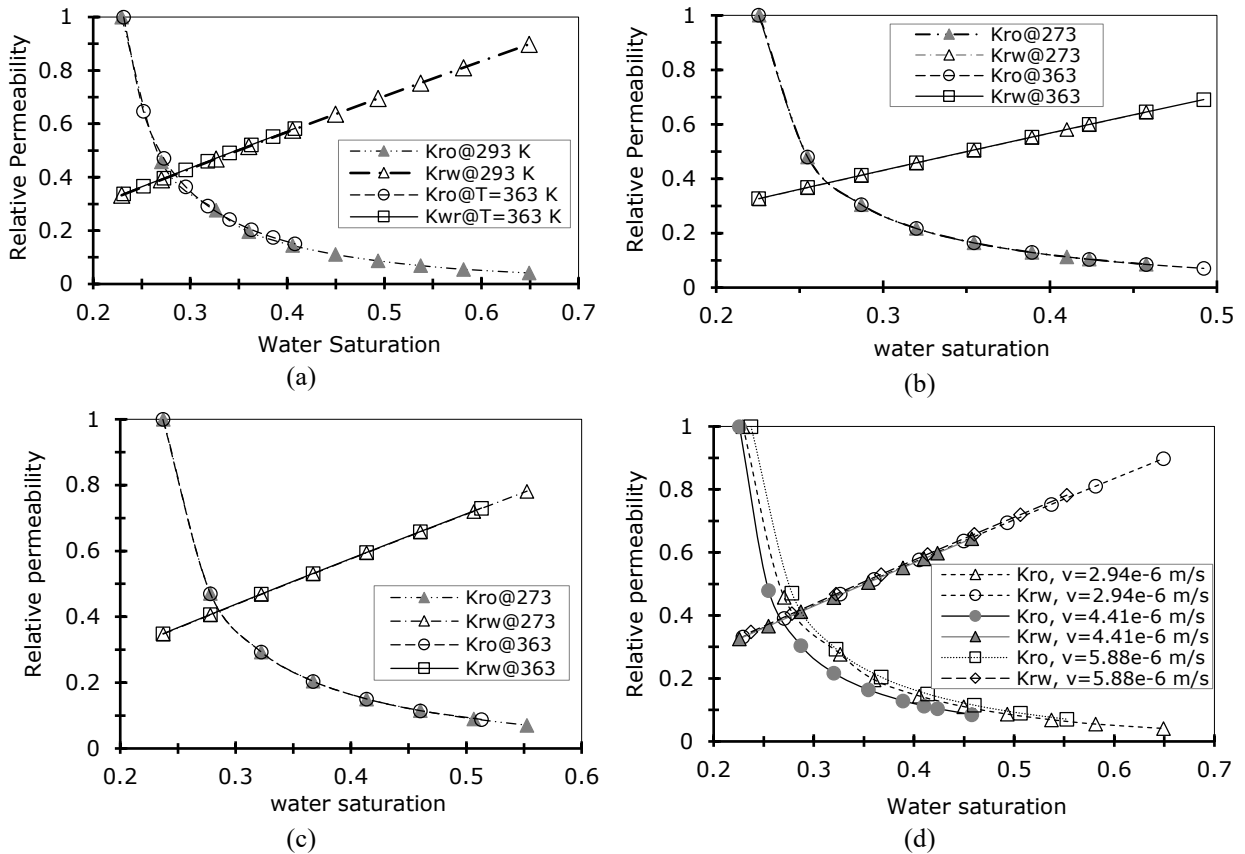


Figure 5: Water saturation along the length of the sample with time.

401
402

403 5.2. Temperature and injection velocity impact on oil-water multiphase the relative permeability

404 Figure 6 compares the relative permeability of oil-water (two phases) at two distinct temperatures of 293 and
 405 363 K. Three different injection rates were employed for each of the temperatures, and the results for relative
 406 permeability are shown in Figure 6 (a-c). It can be seen that the trend of the curves does not alter significantly as
 407 the temperature rises. As a result, the relative permeability curves are insensitive to temperatures between 293 and
 408 363 K. This could be due to the relative permeability of the oil shifting until an ideal temperature is achieved
 409 somewhere between 313 and 323 K, after which the trend reverses as the temperature rises further. This optimal
 410 temperature is known as the "viscous limit." In their experimental study to examine the effect of temperature on
 411 three-phase relative permeability isoperms in heavy oil systems, Akhlaghinia et al. [20] acknowledged this
 412 behaviour.



413 Figure 6 (a-c): Comparison between results of relative permeability at different temperature. (d) Comparison of
 414 relative permeability for different injection velocities.
 415

416 Figure 6d shows the influence of injection velocity on the oil-water relative permeability. The sensitivity of
 417 the phase relative permeability to injection velocities was investigated using three distinct injection velocities of
 418 2.94×10^{-6} m/s, 4.41×10^{-6} m/s, and 5.88×10^{-6} m/s. The water relative permeability curves indicate no significant
 419 change with changes in the injection flow rate for the three distinct flow rates evaluated, however the oil relative
 420 permeability curves show some sensitivity with changes in the injection flow rate. This is similar to the findings
 421 of Sandberg et al [45] that attributed this occurrence to the tendency for the oil phase to flow in slugs. The highest
 422 flow rate caused a shift in relative permeability to the right, while the lowest is linked to the flow rate's median
 423 value. The relationship between relative permeability and flow rate is clearly visible in these results. Because
 424 relative permeability curves reflect a liquid's ability to flow in the presence of another fluid, higher oil relative
 425 permeability is necessary to improve oil phase displacement by water. Higher flow rates are also desirable for
 426 viscous oils in order to improve their relative permeability in relation to the water phase, according to the findings.
 427 Furthermore, flow rate has an impact on residual saturation levels, as an increase in injection flow rate resulted in
 428 a decrease in residual oil saturation but an increase in irreducible water saturation.
 429

430 6. Conclusion

431 The goal of this research is to establish a complete numerical approach for modelling oil-water flow and heat
 432 transfer in porous media with water injection operations. In the simulation, a modified variation of the Eulerian
 433 mixture model was used, while the porous media were modelled using a physical velocity formulation. A viscous
 434 loss term based on Darcy's law without an inertial loss term was used to describe the resistance sink, which is the
 435 source term in the momentum equation. The approach used simulated oil displacement by water at high
 436 temperatures, simulating the conditions of a core flood experiment in the lab. The results were remarkably similar
 437 to the experimental data. The following conclusions can be drawn based on the results and analysis presented.

- 438 i. The macroscopic properties of a porous media, such as relative permeability, can be estimated using a
 439 Computational Fluid Dynamics technique.
- 440 ii. Permeability (relative) Oil flow curves are impacted by flow rate, whereas water relative permeability
 441 has little or no effect.

- 442 iii. The injection flow rate has a major effect on the residual saturations of oil and water, as well as their
443 effective permeability.
444 iv. For temperature ranges of 20 to 90 °C, relative permeability has no discernible sensitivity. However,
445 more research at higher temperatures is needed to determine how temperature affects relative
446 permeability.
447
448

449 **Conflict of Interest:** The authors declare that they have no conflict of interest.
450
451

452 **References**

453

- [1] F. Hussain and Y. Cinar, "Comparison of methods for drainage relative permeability estimation from displacement tests," *Society of Petroleum Engineers*, 2010.
- [2] A. Alizadeh and M. Piri, "The effect of saturation history on three-phase relative permeability: An experimental study," *Water Resources Research*, vol. 50, no. 2, pp. 1636-1664, 2014.
- [3] S. Granet, P. Fabrie, P. Lemonnier and M. Quintard, "A two-phase flow simulation of a fractured reservoir using a new fissure element method," *Journal of Petroleum Science and Engineering*, vol. 32, no. 1, pp. 35-52, 2001.
- [4] G. Di-Donato, Z. Tavassoli and M. J. Blunt, "Analytical and numerical analysis of oil recovery by gravity drainage," *Journal of Petroleum Science and Engineering*, vol. 54, no. 1, pp. 55-69, 2006.
- [5] J. K. Arthur, O. Akinbobola, S. Kryuchkov and A. Kantzas, "Thermal Conductivity Measurements of Bitumen Bearing Reservoir Rocks," in *SPE Canada Heavy Oil Technical Conference. Society of Petroleum Engineers*, 2015.
- [6] A. Afsharpoor and M. Balhof, "Static and dynamic CFD modeling of viscoelastic polymer: trapped oil displacement and deformation at the pore-level," in *SPE annual technical conference and exhibition*, 2013.
- [7] J. Xing, Z. Liu, P. Huang, C. Feng, Y. Zhou, R. Sun and S. Wang, "CFD validation of scaling rules for reduced-scale field releases of carbon dioxide," *Applied Energy*, p. 525-530, 2014.
- [8] Y. Zhao, Z. Liu, X. Shi, X. Qian, Y. Zhou, D. Zhang and Q. Li, "Numerical simulation on BLEVE mechanism of supercritical carbon-dioxide," *Energy Procedia*, 2015.
- [9] H. S. Liang, C. H. Lee, J. W. Wang, C. L. Huang, S. L. Lin, T. K. Huang, W. Z. Wu and T. L. Chen, "Acquisition and analysis of transient data through unsteady-state core flooding experiments," *J Petrol Explor Prod Technol*, vol. 7, no. 1, p. 55-68, 2017.
- [10] H. Nekouie, J. Cao, L. James and T. Johansen, "Analytical Gas-Oil Relative Permeability Interpretation Method for Immiscible Flooding Experiments under Constant Differential Pressure Conditions," in *International Symposium of the Society of Core Analysts*, Snow Mass, Colorado, 2016.
- [11] J. Schembre and A. Kovscek, "A technique for measuring two-phase relative permeability in porous media via X-ray CT measurements," *Journal of Petroleum Science and Engineering*, vol. 39, no. 1, pp. 159-174, 2003.
- [12] M. Oak, "Three-phase relative permeability of water-wet Berea," in *SPE/DOE Enhanced Oil Recovery Symposium*, 1990.
- [13] D. Maloney and A. Brinkmeyer, "Three-phase permeabilities and other characteristics of 260-mD fired Berea," National Inst. for Petroleum and Energy Research, Bartlesville, OK (United States), 1992.
- [14] K. Li, P. Shen and T. Qing, "A New Method for Calculating Oil-Water Relative Permeabilities with Consideration of Capillary Pressure," *Mechanics and Practice*, vol. 16, no. 2, pp. 46-52, 1994.
- [15] M. Singh, V. Mani, M. M. Honarpour and K. K. Mohanty, "Comparison of viscous and gravity dominated gas-oil relative permeabilities," *Journal of Petroleum Science and Engineering*, vol. 30, no. 2, p. 67-81, 2001.
- [16] E. F. Johnson, D. P. Bossler and V. O. Naumann, "Calculation of relative permeability from displacement experiments," *Petroleum Transaction, AIME*, pp. 370-372, 1959.
- [17] H. Arshad, H. J. Sufi, J. Ramey and E. B. William, "Temperature Effects on Relative Permeabilities of Oil-Water," in *57th Annual Fall Technical Conference and Exhibition of the Society of Petroleum Engineers of AIME*, New Orleans, LA, 1982.

- [18] M. A. Miller and J. H. Ramey, "Effect of temperature on oil/water relative permeabilities of unconsolidated and consolidated sands," *Society of Petroleum Engineers Journal*, vol. 25, no. 06, pp. 945-953, 1985.
- [19] Z. Lie-hui, T. Jing, X. Yu and Z. Yu-long, "Effect of temperature on the oil–water relative permeability for sandstone reservoirs," *International Journal of Heat and Mass Transfer*, vol. 105, pp. 535-548, 2017.
- [20] M. Akhlaghinia, F. Torabi and C. Chan, "Experimental investigation of temperature effect on three-phase relative permeability isoperms in heavy oil systems," *Fuel*, vol. 118, pp. 281-290, 2014.
- [21] D. Bennion, F. Thomas, B. Schulmeister and T. Ma, "Correlation of the Low and High Temperature Water-Oil Relative Permeability Characteristics of Typical Western Canadian Unconsolidated Bitumen Producing Formations," in *Canadian International Petroleum Conference*, 2006..
- [22] F. N. M. Torabi and Z. Ostap, "Predicting heavy oil/water relative permeability using modified Corey-based correlations," *Fuel*, vol. 163, pp. 196-204, 2016.
- [23] S. S. Behnam, R. Fariborz and B. Tayfun, "Temperature effects on the heavy oil/water relative permeabilities of carbonate rocks," *Journal of Petroleum Science and Engineering*, vol. 59, no. 1, p. 27–42, 2007.
- [24] S. Esmacili, S. Hemanta, H. Thomas and M. Brij, "Two-phase bitumen/water relative permeability at different temperatures and SAGD pressure: Experimental study," *Fuel*, vol. 276, 2020.
- [25] S. Esmacili, S. Hemanta, H. Thomas and M. Brij, "Effect of Temperature on Bitumen/Water Relative Permeability in Oil Sands," *Energy Fuels*, vol. 34, pp. 12314-12329, 2020.
- [26] S. Esmacili, M. Jafar, S. Hemanta, H. Thomas and M. Brij, "Effect of temperature on relative permeability – Role of viscosity ratio," *Fuel*, vol. 278, 2020.
- [27] S. Esmacili, S. Hemanta, H. Thomas and M. Brij, "Review of the effect of temperature on oil-water relative permeability in porous rocks of oil reservoirs," *Fuel*, vol. 91, no. 116, 2019.
- [28] Y.-S. Wu, "Flow-Governing Equations and Mathematical Models," in *Multiphase Fluid Flow in Porous and Fractured Reservoirs*, Elsevier Inc., 2016, p. 29.
- [29] F. Z. P. A. H. R. Doster, "Numerical solutions of a generalized theory for macroscopic capillarity," *The American Physical Society*, vol. 3, no. 13, 2010.
- [30] S. H. S. Joodat, K. B. Nakshatrala and R. Ballarini, "Modeling flow in porous media with double porosity/permeability: A stabilized mixed formulation, error analysis, and numerical solutions," *Computational & Applied Mechanics Laboratory*, 2017.
- [31] A. Jafari, H. Mohammadreza and G. Reza, "Application of CFD technique to simulate enhanced oil recovery processes: current status and future opportunities," *Petroleum Science*, 2019.
- [32] T. Glatzel, C. Litterst, C. Cupelli, T. Lindemann, C. Moosmann, R. Niekrawietz, W. Streule, R. Zengerle and P. Koltay, "Computational Fluid Dynamics (CFD) software tools for microfluidic applications—A case study," *Computers & Fluids*, vol. 37, no. 3, pp. 218-235, 2008.
- [33] H. Li, S. A. Vasquez and M. Azhar, "Modeling of Multiphase Flows in Porous Media With Applications to Reservoir and Well Performance Analysis," in *Fluids Engineering Division Summer Meeting collocated with the ASME 2016 Heat Transfer Summer Conference and the ASME 2016 14th International Conference on Nanochannels, Microchannels, and Minichannels*, 2016.
- [34] G. Wells, T. Hooijkaas and X. Shan, "Modelling temperature effects on multiphase flow through porous media," *Philosophical Magazine*, vol. 88, no. 28-29, pp. 3265-3279, 2008.
- [35] R. Dias, D. Chalhub, L. Sphaier, T. De Oliveira and P. Fernandes, "Analysis of Oil Displacement Through Water in Porous Media Using Integral Transforms and CFD Package," in *14 th Brazilian Congress of Thermal Sciences and Engineering*, 2012..
- [36] Y.-S. Wu, "Flow-Governing Equations and Mathematical Models," in *Multiphase Fluid Flow in Porous and Fractured Reservoirs*, Elsevier Inc., 2016, pp. 31-34.
- [37] A. Inc., "ANSYS Fluent 14.5.," 2013.
- [38] Z. Xianmin, A.-O. Fawaz and K. Sunil, "Relative Permeability Characteristics and Wetting Behavior of Supercritical CO₂ Displacing Water and Remaining Oil for Carbonate Rocks at Reservoir Conditions," *Energy & Fuels*, 2019.
- [39] M. G. Dezfally, A. Jafari and R. Gharibshahi, "CFD simulation of enhanced oil recovery using nanosilica/supercritical CO₂," *Advanced materials research*, 2015.

- [40] R. Gharibshahi, A. Jafari and H. Ahmadi, "CFD investigation of enhanced extra-heavy oil recovery using metallic nanoparticles/steam injection in a micromodel with random pore distribution," *Journal of Petroleum Science Engineering*, vol. 174, pp. 374-383, 2019.
- [41] S. K. Nandwani, M. Chakraborty and S. Gupta, "Chemical flooding with ionic liquid and nonionic surfactant mixture in artificially prepared carbonate cores: a diffusion controlled CFD simulation," *Journal of Petroleum Science and Engineering*, vol. 173, p. 834843, 2019.
- [42] P. Mohammadmoradi, A. Behrang and A. Kantzas, "Effective Thermal and Electrical Conductivity of Two-Phase Saturated Porous Media," in *SPE Canada Heavy Oil Technical Conference. Society of Petroleum Engineers*, 2016.
- [43] Y. Ahmadi, M. Hassanbeygi and R. Kharrat, "The Effect of Temperature and Injection Rate during Water Flooding Using Carbonate Core Samples: An Experimental Approach," *Iranian Journal of Oil & Gas Science and Technology*, vol. 5, no. 4, pp. 18-24, 2016.
- [44] F. S. Mobeen and S. Mehran, "Relative permeabilities hysteresis for oil/water, gas/water and gas/oil systems in mixed-wet rocks," *Journal of Petroleum Science and Engineering*, vol. 161, pp. 559-581, 2018.
- [45] C. Sandberg and L. Gournay, "The Effect of Fluid-Flow Rate and Viscosity on Laboratory Determinations of Oil-Water Relative Permeabilities," *Trans., AIME*, vol. 213, pp. 36-43, 1958.

454
455